

Coupled multimode optomechanics in the microwave regime

Georg Heinrich and Florian Marquardt

Arnold Sommerfeld Center for Theoretical Physics,

Center for NanoScience and Department of Physics,

Ludwig-Maximilians-Universität München, Theresienstr. 37, D-80333 München, Germany

Institut für Theoretische Physik, Universität Erlangen-Nürnberg, Staudtstr. 7, 91058 Erlangen, Germany

(Dated: July 15, 2021)

The motion of micro- and nanomechanical resonators can be coupled to electromagnetic fields. This allows to explore the mutual interaction and introduces new means to manipulate and control both light and mechanical motion. Such optomechanical systems have recently been implemented in nanoelectromechanical systems involving a nanomechanical beam coupled to a superconducting microwave resonator. Here, we propose optomechanical systems that involve multiple, coupled microwave resonators. In contrast to similar systems in the optical realm, the coupling frequency governing photon exchange between microwave modes is naturally comparable to typical mechanical frequencies. For instance this enables new ways to manipulate the microwave field, such as mechanically driving coherent photon dynamics between different modes. In particular we investigate two setups where the electromagnetic field is coupled either linearly or quadratically to the displacement of a nanomechanical beam. The latter scheme allows to perform QND Fock state detection. For experimentally realistic parameters we predict the possibility to measure an individual quantum jump from the mechanical ground state to the first excited state.

PACS numbers: 85.85.+j, 84.40.Dc, 42.50.Dv

Introduction. - Significant interest in the interaction and dynamics of systems comprising micro- and nanomechanical resonators coupled to electromagnetic fields, as well as the prospect to eventually measure and control the quantum regime of mechanical motion, has stimulated the rapidly evolving field of optomechanics (see [1] for a recent review). In the standard setup, the light field, stored inside an optical cavity, exerts a radiation pressure force on a movable end-mirror whose motion changes the cavity frequency and thus acts back on the photon dynamics. This way, the photon number inside the optical mode is linearly coupled to the displacement of a mechanical object. Beyond the standard approach, new developments have introduced optical setups with multiple coupled light and vibrational modes pointing the way towards integrated optomechanical circuits [2–6]. These systems allow to study elaborate interactions between mechanical motion and light such as mechanically driven coherent photon dynamics that introduces the whole realm of driven two- and multi-level systems to the field of optomechanics [7]. Coupled multimode setups furthermore allow to increase measurement sensitivity [8] and enable fundamentally different coupling schemes. Accordingly, recent experiments achieved coupling the photon number to the square and quadruple of mechanical displacement [2, 9]. Such different coupling schemes are needed, for instance, to afford quantum non-demolition (QND) Fock state detection of a mechanical resonator [2, 10–12].

Besides optics, recent progress has made it possible to realize optomechanical systems in the microwave regime [13, 14]. In this case the optical cavity is replaced by a superconducting microwave resonator whose central con-

ductor capacitively couples to the motion of a nanomechanical beam. This optomechanical approach constitutes a new path to perform on-chip experiments measuring and manipulating nanomechanical motion that adds to electrical concepts using single electron transistors [15–17], superconducting quantum interference devices [18, 19], driven RF circuits [20] or a Cooper-pair box [21, 22]. One advantage of on-chip optomechanics is to use standard bulk refrigerator techniques in addition to laser cooling schemes [23, 24]. This recently enabled cooling a single vibrational mode close to the quantum mechanical ground state [25]. Furthermore, nonlinear circuit elements can be integrated. This afforded ultrasensitive displacement measurements with measurement imprecision below that at the standard quantum limit [26].

Here we go beyond single mode systems, that have been considered for optomechanics in the microwave regime so far, and propose setups with coupled microwave resonators. For these systems, the coupling frequency between microwave modes turns out to be comparable to the mechanical frequency. This has several implications both for the classical and the prospective quantum regime. As an example, focusing on the currently in experiments accessible regime of classical motion, we demonstrate how this allows to manipulate the microwave field in terms of mechanical driving.

Two-resonators setup with linear mechanical coupling. - We consider the coplanar device geometries depicted in Fig. 1a with two identical superconducting microwave resonators a_L , a_R . The central conductors of a_L and a_R are assumed to adjoin for a length d_g that is much smaller than the total wave guides' length

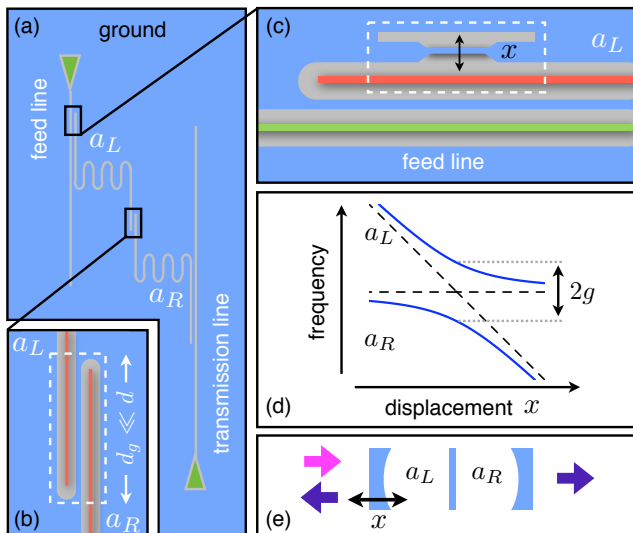


FIG. 1. Schematic device geometry for two superconducting microwave resonators a_L , a_R with a nanomechanical beam coupled to a_L . (a) The two resonators (each of length d) are coupled to external feed and transmission lines (green). (b) The central conductors of a_L and a_R (red) capacitively couple due to a small region of length d_g where the resonators adjoin. (c) At the other end of a_L a small mechanical beam, connected to ground (blue), is placed. Its displacement x affects the line capacitance of resonator a_L changing its resonance frequency. (d) System's resonance frequency as function of displacement: the beam's displacement x linearly changes the bare mode frequency of a_L while the one of a_R is unaffected (dashed). Due to the coupling g between modes there is an avoided crossing $2g$ in the eigenfrequencies (blue). (e) Analogous optical setup: a static, dielectric membrane, placed inside a cavity with a movable mirror, couples two separate optical modes a_L , a_R .

d [Fig. 1b]. A nanomechanical beam, connected to the ground plane, is placed at the other end of a_L [Fig. 1c]. Its motion in terms of displacement x changes the line capacitance c (capacitance per unit length) between the central conductor and the ground plane in a small region. In the following, we will derive and discuss the Hamiltonian for the system depicted in Fig. 1 starting from a single microwave resonator whose line capacitance is changed due to the motion of a mechanical beam [Fig. 1b] [13, 23, 25].

Single MW resonator coupled to a nanomechanical beam. - We concentrate on one of the microwave resonators in Fig. 1. The Lagrangian of an electric circuit can be conveniently expressed in terms of a flux variable $\phi(x, t) \equiv \int_{-\infty}^t d\tau V(x, \tau)$, where $V(x, t) = \partial_t \phi(x, t)$ is the voltage on the transmission line at position x and time t , see for instance [27]. For a finite length microwave resonator with line inductance l and line capacitance c (both per unit length), the corresponding Euler-Lagrange equation yields a wave equation with speed $v = \sqrt{1/lc}$. Using appropriate boundary conditions, $\phi(x, t)$ can be ex-

panded into normal modes ϕ_k , see [28]. The Lagrangian reads $\mathcal{L} = \sum_k [\frac{c}{2} \dot{\phi}_k^2 + \frac{1}{2l} (\frac{k\pi}{d})^2 \phi_k^2]$ and the microwave resonator possesses resonance frequencies $\omega_k = k\pi v/d$. The Hamiltonian is obtained by Legendre transformation using the canonically conjugated momentum $\pi_k = c\dot{\phi}_k$. Quantizing the system by introducing creation and annihilation operators a_k^\dagger , a_k for the individual modes k , with $[a_k, a_{k'}^\dagger] = \delta_{k,k'}$, the Hamiltonian is a sum of harmonic oscillators, $\sum_k \hbar\omega_k a_k^\dagger a_k$, where we neglected the vacuum energy.

For the resonator a_L in Fig. 1, the motion of the mechanical beam will change the line capacitance c at the end of the wave guide. If we denote the total capacitance between the central conductor and the beam by C_b and define the optomechanical frequency pull per displacement, $\epsilon_k = -\partial\omega_k/\partial x$, we find

$$\epsilon_k = \frac{\partial C_b}{\partial x} \cdot Z \cdot \omega_k^2 / (2\pi k), \quad (1)$$

where we used the line impedance $Z = \sqrt{l/c}$. Up to linear order in x , the Hamiltonian for a single microwave resonator coupled to a nanomechanical beam reads $\mathcal{H} = \sum_k \hbar(\omega_{k,0} - \epsilon_k x) a_k^\dagger a_k$.

Coupled MW resonators. - We now turn to the coupled resonator setup in Fig. 1. As the length d_g of the region where a_L and a_R adjoin is much smaller than the resonators' length d , the capacitive coupling between both central conductors can be considered in terms of a constant, total capacitance G . We briefly switch to a discretized description. If we neglect the motion of the nanomechanical beam the circuit diagram looks as depicted in Fig. 2, where the flux variable $\phi(x, t)$ is discretized as $\phi_n(t)$ at position $x = na$, with a being the constant spacing between nodes. For each individual node, an equation of motion can be written down [27]. From this, taking into account appropriate boundary conditions for $a \rightarrow 0$, the continuous version of the corresponding Lagrangian is found to be

$$\begin{aligned} \mathcal{L} = & \sum_k \left[\frac{c}{2} \dot{\phi}_{L,k}^2 - \frac{1}{2l} \left(\frac{k\pi}{d} \right)^2 \phi_{L,k}^2 \right] \\ & + \sum_k \left[\frac{c}{2} \dot{\phi}_{R,k}^2 - \frac{1}{2l} \left(\frac{k\pi}{d} \right)^2 \phi_{R,k}^2 \right] \\ & + \frac{G}{d} \left(\sum_k \dot{\phi}_{R,k} - \sum_k \dot{\phi}_{L,k} \right)^2, \end{aligned} \quad (2)$$

where $\phi_{L,k}$, $\phi_{R,k}$ refer to the individual normal modes of the left and right resonator, respectively. The first two terms describe two separate wave guides, while the last term characterizes the coupling between both.

To transform to the Hamiltonian, we consider the canonically conjugated momentum $\pi_{L[R],k} = \partial\mathcal{L}/\partial\dot{\phi}_{L[R],k} = c\dot{\phi}_{L[R],k} \mp 2\frac{G}{d}(\sum_k \dot{\phi}_{R,k} - \sum_k \dot{\phi}_{L,k})$. In the following we will restrict to a single mode in each

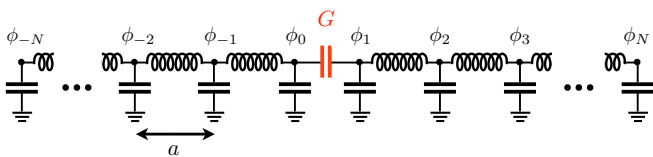


FIG. 2. Discretized circuit diagram for the system depicted in Fig. 1 without nanomechanical beam. The two central conductors are coupled via a total capacitance G . l and c are the line inductance and capacitance, respectively. a is the spacing between discrete points.

resonator ($k = 1$), and drop the label referring to the mode index. For $G/d \ll c$ (see discussion below), we can simplify the expression for $\pi_{L[R],k}$ and consider $\pi_{L[R],k} = c\dot{\phi}_{L[R],k}$. The first two terms of (2) transform into two harmonic oscillators of frequency ω_L and ω_R . For the coupling we have to consider $(\dot{\phi}_R - \dot{\phi}_L)^2$ with $\dot{\phi}_{L[R]} = \pi_{L[R]}/c = i\sqrt{\frac{\hbar\omega_{L[R]}}{2c}}(a_{L[R]}^\dagger - a_{L[R]})$, see [28]. Using rotating wave approximation, we find the Hamiltonian,

$$\mathcal{H} = \hbar\omega_L \left(1 - \frac{G}{dc}\right) a_L^\dagger a_L + \hbar\omega_R \left(1 - \frac{G}{dc}\right) a_R^\dagger a_R + \hbar\sqrt{\omega_L\omega_R} \frac{G}{dc} (a_L^\dagger a_R + a_R^\dagger a_L),$$

where we neglected the vacuum energy. Note that none of the resonators in Fig. 1 is short-circuited such that there are voltage antinodes at both ends of each resonator allowing to have maximal coupling between a_L and a_R , as well as to the feed and transmission line.

The coupling between the resonators has two effects. First, both frequencies ω_L , ω_R , originally defined for uncoupled modes, are lowered by a constant value. In the following, this shift of frequency is neglected by simply redefining the resonators' frequencies. More important is the coupling between modes in terms of the coupling frequency

$$g = \sqrt{\omega_L\omega_R} \frac{G}{dc}. \quad (3)$$

Finally we take into account the motion of the nanomechanical beam changing the left mode's bare eigenfrequency ω_0 in the way discussed above, $\omega_L(x) = \omega_0 - \epsilon x$ (see Eq. (1) with $k = 1$). The final Hamiltonian for the system depicted in Fig. 1 then reads

$$\mathcal{H} = \hbar(\omega_0 - \epsilon x) a_L^\dagger a_L + \hbar\omega_0 a_R^\dagger a_R + \hbar g (a_L^\dagger a_R + a_R^\dagger a_L). \quad (4)$$

In principle, according to (3) with $\omega_L(x)$, the coupling frequency g depends on displacement x . However, for typical parameters the dependence is negligible and g can be considered to be constant. The resonance frequency of (4) is depicted in Fig. 1d.

Coupling frequency comparable to the mechanical frequency ($g \simeq \Omega$). - Given Eq. (3), the coupling frequency between the two resonator modes reads $g/\omega_0 = (c_g/c) \cdot (d_g/d)$, where we defined the coupling line capacitance $c_g = G/d_g$ along the length of the coupling region d_g . In general, c_g will be much smaller than the line capacitance between each central conductor and the ground plane c : first of all, the distance between the two central conductors is significantly larger than the distance between a single conductor and the adjacent ground plane. Second, the capacitance between the central strip lines is shielded by the grounded region in between. Here we crudely assume $c_g/c = 10^{-2}$. For d in the cm range and $d_g \simeq 0.1\text{mm}$ (d_g is chosen such that a several $10\mu\text{m}$ long nanomechanical beam can be fabricated in between the region where the resonators align), we have $d_g/d = 10^{-2}$ and the coupling between modes is $g/\omega_0 = 10^{-4}$ where ω_0 will be in the GHz range. Common eigenfrequencies of nanomechanical beams are $\Omega = 100\text{kHz} - 10\text{MHz}$. Hence, due to their much smaller photon frequency, coupled multimode optomechanical systems in the microwave regime naturally possess coupling frequencies in the range of typical mechanical frequencies ($g \simeq \Omega$). The relevance of this regime for instance to realize all kinds of driven two- and multi-level photon dynamics in optomechanical systems has been pointed out in [7].

Transmission spectrum. - As an example to emphasize the characteristics of coupled optomechanical systems in the microwave regime and to demonstrate implications of $g \simeq \Omega$ even in the presently accessible regime of classic mechanical motion, we will discuss how the microwave field in the setup of Fig. 1 can be manipulated in terms of mechanical driving (see [29] for a universal mechanical actuation scheme). Experimentally, the impact can be most easily observed in terms of the transmission spectrum. We assume the left resonator a_L to be driven at frequency ω_L via the feed line, while the transmission down the transmission line is recorded. We consider the coupling of the left (right) resonator to the feed (transmission) line in terms of the resonators' decay rate κ . Given the Hamiltonian (4), using input/output theory, the equation of motion for the averaged fields $\alpha_L = \langle a_L \rangle$, $\alpha_R = \langle a_R \rangle$ read

$$\begin{aligned} \frac{d}{dt}\alpha_L &= \frac{1}{i}(-\epsilon x(t)\alpha_L + g\alpha_R) - \frac{\kappa}{2}\alpha_L - \sqrt{\kappa}b_L^{in}(t) \\ \frac{d}{dt}\alpha_R &= \frac{1}{i}g\alpha_L - \frac{\kappa}{2}\alpha_R, \end{aligned} \quad (5)$$

where $b_L^{in}(t) = e^{-i\Delta_L t}b^{in}$ describes the electromagnetic drive along the feed line with amplitude b^{in} and frequency ω_L . Here we used a rotating frame with laser detuning from resonance $\Delta_L = \omega_L - \omega_0$. The transmission $T(t) =$

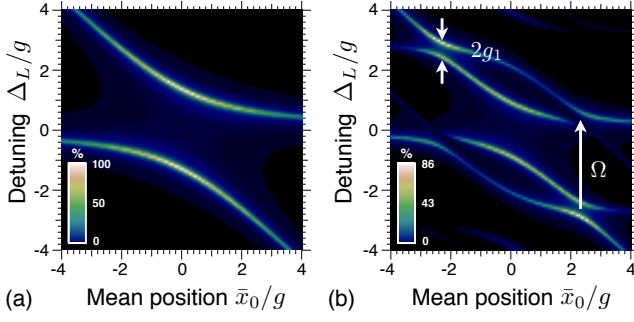


FIG. 3. Transmission spectrum for the setup depicted in Fig. 1 for resonators' decay rate $\kappa = 0.1g$: density plot for the time-averaged transmission depending on mean mechanical displacement $\bar{x}_0 = \epsilon x_0$, and frequency detuning $\Delta_L = \omega_L - \omega_0$ of the feed line's microwave drive at ω_L (ω_0 denotes the left mode's bare frequency for $x = 0$). (a) Without mechanical drive ($x(t) = x_0$); the spectrum is given by the resonance frequency depicted in Fig. 1d. (b) For mechanical driving ($x(t) = A \cos(\Omega t) + x_0$) with amplitude $\bar{A} = \epsilon A = 1.5\Omega$ and frequency $\Omega = 3g$; mechanical sidebands displaced by Ω appear and intersect the original photon branches where, due to mechanically driven Rabi dynamics, high transmission and additional anticrossings arise. The gap $2g_1$ is determined by the Bessel function J_1 according to $2g_1 = 2gJ_1(\bar{A}/\Omega)$.

$\kappa \langle a_R^\dagger(t) a_R(t) \rangle / (b^{in})^2$ can be expressed as

$$T(t) = \kappa^2 \left| \int_{-\infty}^t G(t, t') e^{-i\Delta_L t' - (\kappa/2)(t-t')} dt' \right|^2, \quad (6)$$

where the phase comprises the feed line's drive and resonators' decay, while the Green's function $G(t, t')$ describes the amplitude for a photon to enter the left resonator's mode a_L at time t' and to be found in the right one a_R later at time t .

We take into account two scenarios: first, the beam is at rest given a constant displacement $x(t) = x_0$; second, the beam is mechanically driven to oscillate with amplitude A and frequency Ω around the mean position x_0 , $x(t) = x_0 + A \cos(\Omega t)$. Fig. 3a shows numerical results of the transmission spectrum without mechanical driving. The spectrum corresponds to the system's resonance frequency depicted in Fig. 1d where the resonance width is set by the resonators' decay rate κ . In contrast, Fig. 3b shows the transmission including mechanical driving with $\Omega = 3g$, i.e. $g \simeq \Omega$ being characteristic for coupled microwave optomechanics.

To understand the main features of Fig. 3b we note that, in general, two processes are involved to observe transmission, see (6): first, the left resonator a_L must be excited by the electromagnetic drive $b_L^{in}(t) = e^{-i\Delta_L t} b^{in}$; second, the internal dynamics must be able to transfer photons from a_L to a_R . From (5) the solution $G(t, t')$ can be found to be

$$G(t, t') = \tilde{\alpha}_R(t, t') e^{-i\phi(t')} \quad (7)$$

where $\phi(t') = (\bar{A}/\Omega) \sin(\Omega t')$ and $\tilde{\alpha}_R(t, t')$ is a solution to the driven two state problem

$$\frac{d}{dt} \begin{pmatrix} \tilde{\alpha}_L \\ \tilde{\alpha}_R \end{pmatrix} = \frac{1}{i} \begin{pmatrix} -\bar{x}_0 & g e^{-i\phi(t)} \\ g e^{+i\phi(t)} & 0 \end{pmatrix} \begin{pmatrix} \tilde{\alpha}_L \\ \tilde{\alpha}_R \end{pmatrix}, \quad (8)$$

with $t \geq t'$ and initial condition $\tilde{\alpha}_L(t', t') = 1$, $\tilde{\alpha}_R(t', t') = 0$. Note that we expressed displacement in terms of frequency; $\bar{A} = \epsilon A$, $\bar{x}_0 = \epsilon x_0$. For $\bar{A} \neq 0$, in addition to the electromagnetic drive (see $e^{-i\Delta_L t'}$ in (6)), the mechanical driving can excite a_L in terms of multiples of the mechanical frequency $m\Omega$. This mechanical excitation is described by the phase factor $e^{-i\phi(t')} = \sum_m J_m(\bar{A}/\Omega) e^{-im\Omega t'}$ in (7) and leads to mechanical sidebands in the spectrum [cf. Fig. 3b]. Note that the individual process $m\Omega$ is described by a Bessel function $J_m(\bar{A}/\Omega)$ and can be tuned by the driving strength. Beyond the modified excitation, the driving significantly changes the internal dynamics of the microwave fields, see Eq. (8). In particular the mechanical motion can initiate mechanically driven Rabi dynamics exchanging photons between a_L and a_R that leads to high transmission if the mechanical drive at Ω is in resonance with the modes' frequency difference. For sufficiently strong driving, the mechanically assisted process leads to additional anticrossings in the spectrum resembling Autler-Townes splittings known from quantum optics (see marker in Fig. 3b). From Eq. (8) we find that the spacing of this first additional splitting scales according to $2gJ_1(\bar{A}/\Omega)$ and can likewise be tuned by the mechanical driving strength. All this illustrates how, due to $g \simeq \Omega$, the microwave field can extensively be manipulated by mechanical motion in terms of mechanically driven coherent photon dynamics.

Coupling to the square of displacement. - We present a modified scheme comprising coupled microwave resonators that allows to couple the photon number to the *square* of mechanical displacement [Fig. 4a-b]. In contrast to the setup in Fig. 1, here the nanomechanical beam is placed in the region *between* the two resonators, such that its motion affects both simultaneously [Fig. 4b]. While for a given displacement x , the line capacitance c of the first resonator is increased, the one of the second wave guide is decreased and vice versa. According to our previous results, using the notation from above, the Hamiltonian for this setup reads

$$H = \hbar(\omega_0 - \epsilon x) a_L^\dagger a_L + \hbar(\omega_0 + \epsilon x) a_R^\dagger a_R + \hbar g (a_L^\dagger a_R + a_R^\dagger a_L), \quad (9)$$

where $g = \omega_0 c_g d_g / cd$, see (3) and (4).

Fig. 4c illustrates the system's resonance frequency $\omega_\pm(x) = \omega_0 \pm \sqrt{g^2 + (\epsilon x)^2}$ as function of displacement. Naturally all the characteristics of coupled multimode optomechanics in the microwave regime, that have been discussed above, apply. In particular the hyperbola-

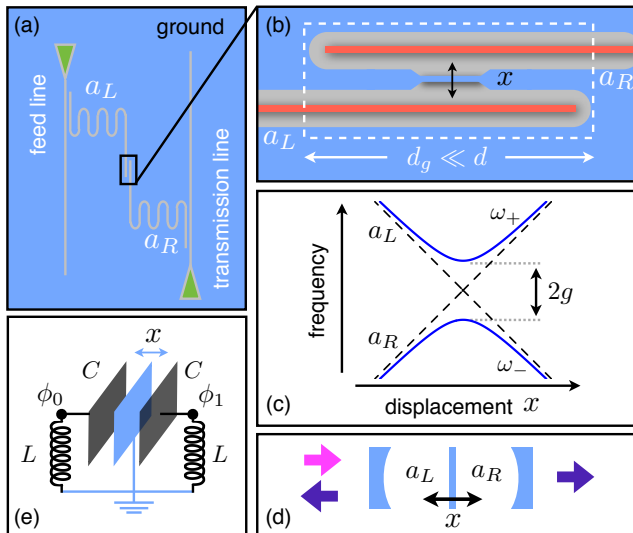


FIG. 4. Schematic device geometry for two microwave resonators a_L , a_R with a nanomechanical device coupled to *both* of them. (a) Two stripline resonators (each of length d) are coupled to external feed and transmission lines (green). The central conductors of a_L , a_R (red) are capacitively coupled in a small region of length d_g where the wave guides adjoin. (b) Between the two resonators a small mechanical beam, connected to ground (blue), is placed. Its displacement x affects the line capacitance of both, a_L and a_R . (c) System's resonance frequency as function of displacement: the beam's displacement linearly changes the bare modes' frequency of a_L and a_R (dashed). Due to the coupling g between the resonators, there is an avoided crossing $2g$ in the eigenfrequencies ω_{\pm} (blue). (d) Analogous optical setup with a movable dielectric membrane placed in the middle of a cavity [2]. (e) Schematic realization with two microwave LC circuits where a central plate is grounded and resonates against two others that build the LC circuits. In the notation of Fig. 2 we get for the coupling frequency $g = \omega_{LC}G/C$ with $\omega_{LC} = 1/\sqrt{LC}$.

shaped avoided level crossing allows to realize Landau-Zener transitions and the dynamics of Landau-Zener-Stueckelberg oscillations in the light field of a microwave setup. At the extrema of $\omega_{\pm}(x)$ the Hamiltonian allows an exclusive coupling to the square of mechanical displacement x^2 . Thus, in the following, we investigate the prospects to perform QND Fock state detection using this microwave setting.

Fock state detection. - In principle, an exclusive coupling of the photon number to x^2 allows to perform QND Fock state detection and to observe quantum jumps of a mechanical resonator [10, 11]. Indeed the Hamiltonian (9) corresponds to the one found for an optical setup (see Fig. 4d), that generated a lot of interest in this regard [2, 12]. We focus on one microwave mode with annihilation operator a and expand the resonance frequency $\omega_+(x)$ around x_0 . For $x_0 = 0$ the linear contribution vanishes and the Hamiltonian reads

$H = \hbar \left(\omega_+(0) + \frac{1}{2} \omega_+''(0) x_{zp}^2 [b^\dagger + b]^2 \right) a^\dagger a + \hbar \Omega b^\dagger b$, where we considered the phonon number operator $n = b^\dagger b$ and quantized $(x - x_0)$ using the mechanical beam's displacement operator $\hat{x} = x_{zp} (b^\dagger + b)$. The zero-point displacement $x_{zp} = \sqrt{\hbar/2m\Omega}$ is determined by the mechanical mass m and frequency Ω . Applying rotating wave approximation (RWA), $(b^\dagger + b)^2 \simeq 2n + 1$, we immediately see that $[H, n] = 0$. For a potential experiment we consider a scheme in analogy to the one proposed for the optical setup [2]. The mechanics is cooled to the quantum mechanical ground state [23, 25]. After switching off the cooling, the phonon number n is measured via the frequency of the microwave mode. To detect a quantum jump from $n = 0$ to $n = 1$, the frequency shift per phonon $\Delta\omega = \omega_+''(0) x_{zp}^2$, where $\omega_+''(0) = \epsilon^2/g$, must be resolved within the lifetime of the phonon ground state $\tau^{(0)}$. Given the imprecision of the frequency measurement in terms of the angular frequency noise power spectral density $S_{\omega\omega}$ (in units s^{-2}/Hz), the signal-to-noise ratio reads $\Sigma = (\Delta\omega)^2 \tau^{(0)} / S_{\omega\omega}$ [2]. In contrast to the optical regime, where shot-noise-limited frequency measurements are routinely achieved, microwave setups in general suffer from amplifier noise adding n_{add} quanta of noise beyond the shot-noise limit in a Pound-Drever-Hall scheme, such that $S_{\omega\omega} = (n_{add} + 1/2) \kappa^2 \hbar \omega_c / 16 P_{in}$ (see [30]). P_{in} denotes the incident power and ω_c is the resonance frequency of the cavity. While commercially available systems add a significant amount of noise, a new Josephson parametric amplifier achieved $n_{add} < 1/2$ [31]. This technique has already been used for displacement measurements in a microwave optomechanical system with $n_{add} = 1.3$ [26]. Essentially, the total lifetime $\tau^{(0)} = 1/(\tau_T^{-1} + \tau_{RWA}^{-1} + \tau_{lin}^{-1})$ is set by the thermal lifetime $\tau_T = \hbar Q / k_B T$ via the mechanical quality factor Q and the chip temperature T . Additional contributions due to the RWA (τ_{RWA}) and imprecise positioning $x_0 \neq 0$ (τ_{lin}) will be determined via Fermi's golden rule rates (see [2]).

For microwave setups using a small nanomechanical beam manufactured close to the central conductor of a stripline resonator, achieving optomechanical couplings of $\epsilon \simeq 1 - 100 \text{ kHz/nm}$ [13, 23, 25], the frequency shift per phonon $\Delta\omega \propto \epsilon^2$ turns out to be extremely small making Fock state detection impossible. A new on-chip microwave system however, consisting of an LC circuit where the plates of a parallel-plate condenser mechanically resonate, achieves $\epsilon = 65 \text{ MHz/nm}$ [32]. Our proposal transfers to this scheme by stacking three such plates, see Fig. 4e. For experimentally realistic parameters [32], a calculation of Σ yields that a setup with this optomechanical coupling would allow to detect an individual quantum jump from the mechanical ground state to the first excited state, see Tab. I. Note that, in contrast to the setup discussed in [2], the parameters here are already in the small-splitting regime $g < \Omega$, and the details of Fock state detection in that regime may require further

ϵ [MHz/nm]	m [pg]	$\Omega/2\pi$ [MHz]	$Q/10^5$	κ/Ω	$g/2\pi$ [MHz]	P_{in} [pW]	x_0 [pm]	n_{add}	T [mK]	Σ
65	10	11	3.5	1/70	0.5	200	0.5	1	20	1.0
70	10	11	5.0	1/100	0.5	50	0.5	1	20	1.2

TABLE I. Two sets of experimental parameters that would allow to observe an individual quantum jump from the mechanical ground state to the first excited state, with a signal-to-noise ratio $\Sigma \geq 1$. Further parameter $\omega_c/2\pi = 5$ GHz.

analysis. Finally, we point out that such a setup, even for $\Sigma < 1$, would allow to measure “phonon shot noise”, i.e. quantum energy fluctuations around an average phonon number, of a mechanically driven, ground-state-cooled mechanical oscillator [33].

Conclusion. - To conclude, we introduced and analyzed theoretically coupled multimode optomechanical systems for the microwave regime. In contrast to the optical domain, these systems possess coupling frequencies between the electromagnetic modes that are naturally in the range of typical mechanical frequencies ($g \simeq \Omega$). By calculating the transmission spectrum, we demonstrated how this allows to manipulate the microwave field dynamics in terms of mechanical driving. In principle $g \simeq \Omega$ enables to realize all kinds of driven two- and multi-level dynamics known from quantum optics in the microwave light field. Our discussion mostly focussed on classical mechanical motion. However, for mechanical oscillators in the quantum regime, coupled multimode systems with $g \simeq \Omega$ will be particularly interesting. For instance it might be possible to realize hybridized states which are superpositions of states with a photon being in different modes and phonons in the mechanics. We furthermore proposed a multimode setup that allows to couple the microwave photon number to the square of mechanical displacement and enables QND Fock state detection. For experimentally realistic parameters we predicted the possibility to detect an individual quantum jump from the mechanical ground state to the first excited state. The same scheme also allows to measure phonon shot noise. Both experiments would constitute a major breakthrough.

We acknowledge fruitful discussions with Rudolf Gross, Eva Weig, John Teufel and Konrad Lehnert as well as support by the DFG (NIM, SFB 631, Emmy-Noether program), GIF and DIP.

[1] F. Marquardt and S. M. Girvin, *Physics*, **2**, 40 (2009)
[2] J. D. Thompson, B. M. Zwickl, A. M. Jayich, F. Marquardt, S. M. Girvin, and J. G. E. Harris, *Nature*, **452**, 72 (2008)
[3] M. Li, W. H. P. Pernice, C. Xiong, T. Baehr-Jones, M. Hochberg, and H. X. Tang, *Nature*, **456**, 480 (2008)
[4] M. Eichenfield, R. Camacho, J. Chan, K. J. Vahala, and O. Painter, *Nature*, **459**, 550 (2009)
[5] M. Eichenfield, J. Chan, R. M. Camacho, K. J. Vahala,

and O. Painter, *Nature*, **462**, 78 (2009)
[6] G. Anetsberger, O. Arcizet, Q. P. Unterreithmeier, R. Riviere, A. Schliesser, E. M. Weig, J. P. Kotthaus, and T. J. Kippenberg, *Nat. Phys.*, **5**, 909 (2009)
[7] G. Heinrich, J. G. E. Harris, and F. Marquardt, *Phys. Rev. A*, **81**, 011801(R) (2010)
[8] J. M. Dobrindt and T. J. Kippenberg, *Phys. Rev. Lett.*, **104**, 033901 (2010)
[9] J. C. Sankey, C. Yang, B. M. Zwickl, A. M. Jayich, and J. G. E. Harris, preprint (2010), arXiv:1002.4158
[10] V. B. Braginsky, Y. I. Vorontsov, and K. S. Thorne, *Science*, **209**, 547 (1980)
[11] V. B. Braginsky, F. Y. Khalili, and K. S. Thorne, *Quantum Measurement* (Cambridge University Press, 1992)
[12] A. M. Jayich, J. C. Sankey, B. M. Zwickl, C. Yang, J. D. Thompson, S. M. Girvin, A. A. Clerk, F. Marquardt, and J. G. E. Harris, *New J. Phys.*, **10**, 095008 (2008)
[13] C. A. Regal, J. D. Teufel, and K. W. Lehnert, *Nat. Phys.*, **4**, 555 (2008)
[14] J. B. Hertzberg, T. Rocheleau, T. Ndukum, M. Savva, A. A. Clerk, and K. C. Schwab, *Nat. Phys.*, **6**, 213 (2010)
[15] R. G. Knobel and A. N. Cleland, *Nature*, **424**, 291 (2003)
[16] M. D. LaHaye, O. Buu, B. Camarota, and K. C. Schwab, *Science*, **304**, 74 (2004)
[17] A. Naik, O. Buu, M. D. Lahaye, A. D. Armour, A. A. Clerk, M. P. Blencowe, and K. C. Schwab, *Nature*, **443**, 193 (2006)
[18] S. Etaki, M. Poot, I. Mahboob, K. Onomitsu, H. Yamaguchi, and H. S. J. van der Zant, *Nat. Phys.*, **4**, 785 (2008)
[19] E. Buks, E. Segev, S. Zaitsev, B. Abdo, and M. P. Blencowe, *Europhys. Lett.*, **81**, 10001 (2008)
[20] K. R. Brown, J. Britton, R. J. Epstein, J. Chiaverini, D. Leibfried, and D. J. Wineland, *Phys. Rev. Lett.*, **99**, 137205 (2007)
[21] M. D. LaHaye, J. Suh, P. M. Echternach, K. C. Schwab, and M. L. Roukes, *Nature*, **459**, 960 (2009)
[22] A. D. O’Connell, M. Hofheinz, M. Ansmann, R. C. Bialczak, M. Lenander, E. Lucero, M. Neeley, D. Sank, H. Wang, M. Weides, J. Wenner, J. M. Martinis, and A. N. Cleland, *Nature*, **464**, 697 (2010)
[23] J. D. Teufel, J. W. Harlow, C. A. Regal, and K. W. Lehnert, *Phys. Rev. Lett.*, **101**, 197203 (2008)
[24] J. D. Teufel, C. A. Regal, and K. W. Lehnert, *New J. Phys.*, **10**, 095002 (2008)
[25] T. Rocheleau, T. Ndukum, C. Macklin, J. B. Hertzberg, A. A. Clerk, and K. C. Schwab, *Nature*, **463**, 72 (2010)
[26] J. D. Teufel, T. Donner, M. A. Castellanos-Beltran, J. W. Harlow, and K. W. Lehnert, *Nat. Nano.*, **4**, 820 (2009)
[27] M. H. Devoret, in *Quantum Fluctuations* (Les Houches Session LXIII, 1995) pp. 351–386
[28] A. Blais, R. S. Huang, A. Wallraff, S. M. Girvin, and R. J. Schoelkopf, *Phys. Rev. A*, **69**, 062320 (2004)
[29] Q. P. Unterreithmeier, E. M. Weig, and J. P. Kotthaus, *Nature*, **458**, 1001 (2009)

- [30] E. D. Black, Am. J. Phys., **69**, 79 (2001)
- [31] M. A. Castellanos-Beltran, K. D. Irwin, G. C. Hilton, L. R. Vale, and K. W. Lehnert, Nat. Phys., **4**, 928 (2008)
- [32] J. D. Teufel and K. W. Lehnert, Priv. communication.
- [33] A. Clerk, F. Marquardt, and J. Harris, preprint (2010), arXiv:1002.3140